Supporting Information

Stable Lithium Deposition Enabled by Acid-Treated g-C_3N_4 Interface Layer for Lithium Metal Anode

Xiaoyu Luan, [a] *Chenggang Wang,* [a] *Chunsheng Wang,* [a] *Xin Gu,* [*b] *Jian Yang* [*a] *and Yitai Qian* [a,c]

[a] Key Laboratory of Colloid and Interface Chemistry, Ministry of Education, School of Chemistry and Chemical Engineering, Shandong University, Jinan, 250100, P. R. China.

[b] Institute of New Energy, College of New Energy, State Key Laboratory of Heavy Oil Processing, China University of Petroleum (East China), Qingdao, 266580, P. R. China.

[c] Hefei National Laboratory for Physical Science at Microscale, Department of Chemistry, University of Science and Technology of China, Hefei, 230026, P. R. China

Corresponding Author:

*E-mail: guxin@upc.edu.cn

*E-mail: yangjian@sdu.edu.cn

Material Characterizations. XRD patterns were measured on an X-ray diffractometer (Bruker D8 advanced, Germany) using graphite-monochromatized Cu Kα radiation. Scanning electron microscopy (SEM) images and energy-dispersive X-ray spectroscopy (EDS) mapping images were obtained on a field-emission scanning electron microscope (ZEISS SUPRA 55, Germany). TEM images were acquired from a transmission electron microscope (JEOL JEM 1011, Japan). Infrared spectra were acquired from a Fourier-transformed infrared spectrometer (FTIR, Bruker Tensor 27, Germany). X-ray photoelectron spectra was obtained by Thermo ESCALAB 250XI with monochromatic Al Ka radiation. Contact angle was acquired on Kruss DSA10 (Germany).

Electrochemical measurements. 2025-type coin cells were used for the assembling of both the symmetric cells and full cells, with Celgard 2400 microporous polypropylene membrane as separator. For the symmetric cells and Li//$LiFePO_4$ full cells, 1M $LiPF_6$ in ethylene carbonate (EC), dimethyl carbonate (DMC) and ethyl methyl carbonate (EMC) (1: 1: 1, v/v/v) containing 2 wt% FEC was employed as electrolyte. For the symmetric cells and Li//S full cells, the electrolyte was 1 M LiTFSI in 1,3-dioxolane (DOL) and 1,2-dimethoxyethane (DME) (1: 1 v/v) with 2 wt% $LiNO_3$. To fabricate $LiFePO_4$ cathode, commercial $LiFePO_4$ (Shandong Yuhuang New Energy Technology Co. Ltd.), acetylene black and polyvinylidene fluoride (PVDF, DodoChem Co.Ltd.) with a weight ratio of 8:1:1 were mixed with NMP and hand-milled for at least 30 minutes in a mortar to obtain a black slurry. The

slurry was then spread on a piece of clean aluminum foil by doctor blade method and dried in vacuum oven at 60 ^{o}C for 12 h. After drying, the loaded Al foil was roll-pressed and punched into discs with 10 mm in diameter. The average mass loading of $LiFePO_4$ was about 7 mg cm^{-2}. The preparation process for S cathode was the same as that of $LiFePO_4$ cathode, using S/graphene and PVDF as raw materials with a weight ratio of 9:1. The mass loading of S was approximately 0.7 mg cm^{-2}. Galvanostatic discharge/charge measuremets were conducted on battery cyclers (LAND CT-2001A, China). Electrochemical impedance spectra (EIS) were obtained from an electrochemical workstation (AUTOLAB PGSTAT302N, Switzerland) in the frequency range of 100 kHz to 0.1 Hz. All the electrochemical tests were carried out at 25 ^{o}C.

Evaluation method of exchange current density:

The exchange current density was calculated by the equation as followed.

$$i \approx i_0 \frac{F\ \eta_{total}}{RT\quad 2}$$

The i_0 is exchange current density, F is the Faraday's constant, R presents gas constant, η_{total} is the total overpotential of symmetric cells. The i_0 could be obtained by the slope of the straight line by ploting the current density i as a function of η_{total}.

Evaluation method of Li ion diffusion coefficient:

The Li ion diffusion coefficient was estimated by the Warburg coefficient, which was obtained by electrochemical impedance spectroscopy of asymmetric cell. The

Nyquist polt turn into a straight line in the low frequency range called Warburg-diffusion element (σ). And the Warburg cofficient σ could be calculated to the slope of diffusion controlled straight line by ploting the Warburg impedance Z as a function of $\omega^{-1/2}$ in the low frequency region. $Z_W = \frac{\sigma}{\sqrt{\omega}} - i\frac{\sigma}{\sqrt{\omega}}$

The Li ion diffusion coefficient (D) is in direct proportion to $\left(\frac{1}{\sigma}\right)^2$. And the equation could be described as followed with the assumption of faster diffusion in the electrolyte:

$$\mathrm{D} = \frac{1}{2}\left[\left(\frac{V_m}{\sigma z F A}\right)\left(\frac{dE}{dx}\right)\right]^2$$

The V_m is the molar volume of the active materials, σ presents the Warburg coefficient, z is the valence state of the diffusing species, F is the Faraday's constant, A is the surface area of the electrode and dE/dx is the gradient of the slope of the gavanostatic discharge curve.

Herein, Li ion diffusion coefficient could be estimated among three kinds of electrodes.

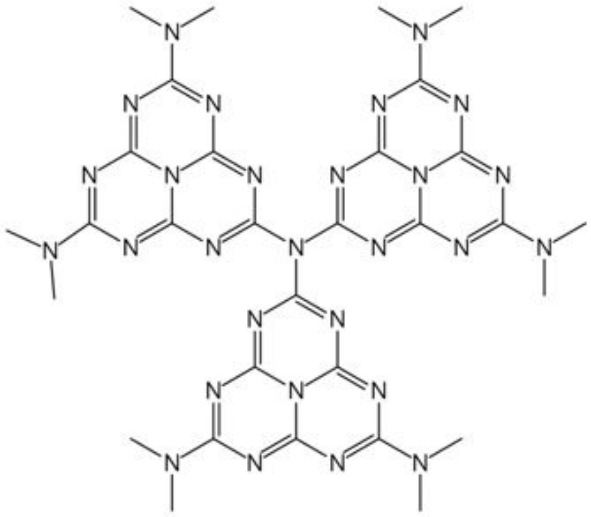

Figure S1. Molecular structure of heptazine-derived repeating units in g-C_3N_4.

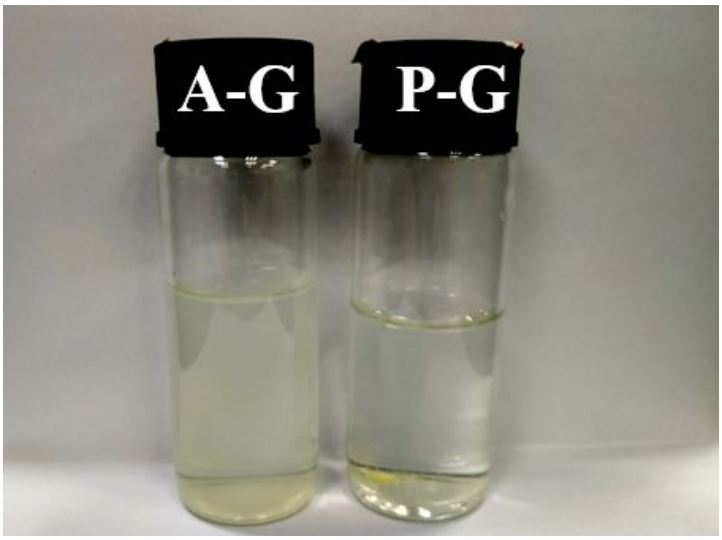

Figure S2. Optical photograph of A-G and P-G dispersed in water.

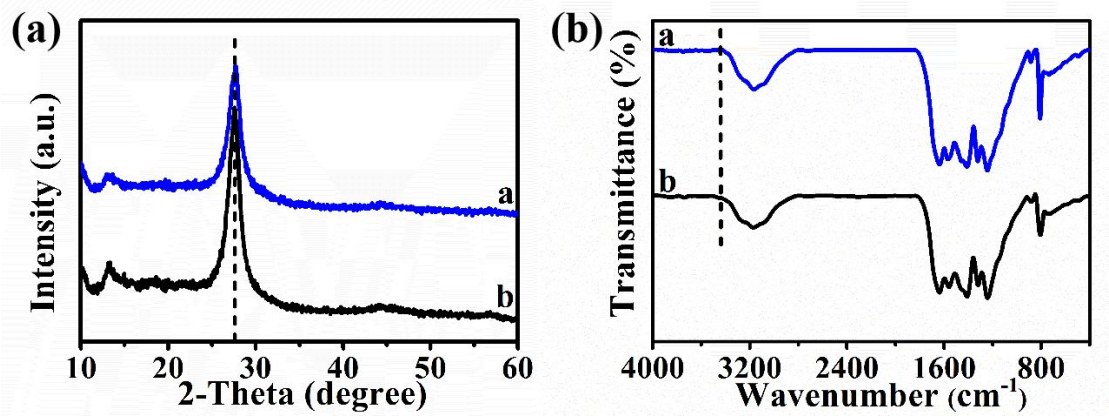

Figure S3. (a) XRD patterns and (b) FTIR spectra of pristine g-C_3N_4 and water-treated g-C_3N_4.

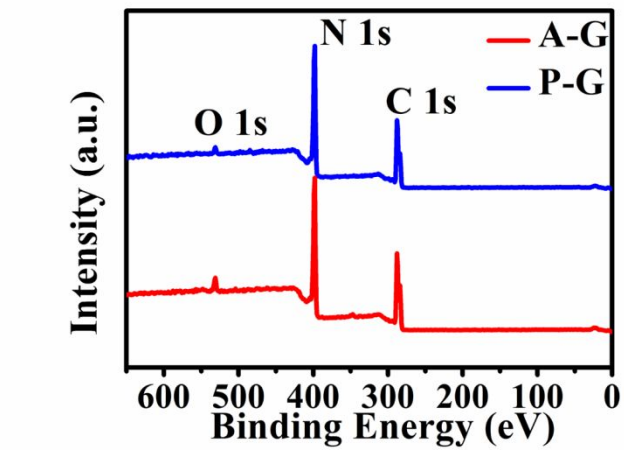

Figure S4. Full XPS spectra of P-G and A-G.

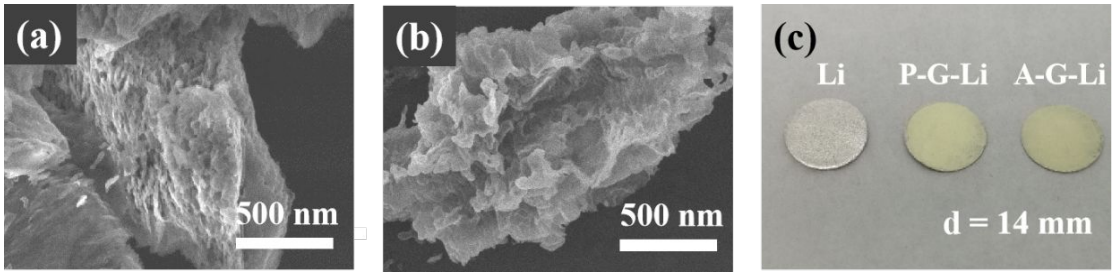

Figure S5. SEM images of (a) P-G and (b) A-G. (c) Optical photograph of pristine Li, P-G-Li, and A-G-Li electrodes.

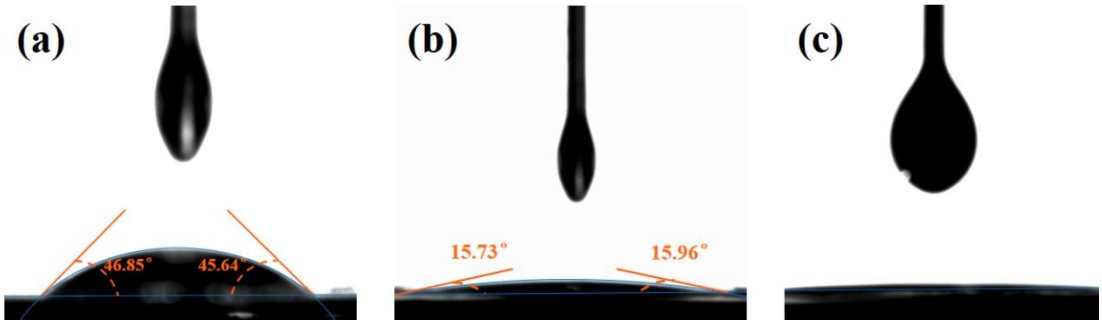

Figure S6. Contact angles of ester-based electrolyte toward pristine Li (a), P-G-Li (b) and A-G-Li (c).

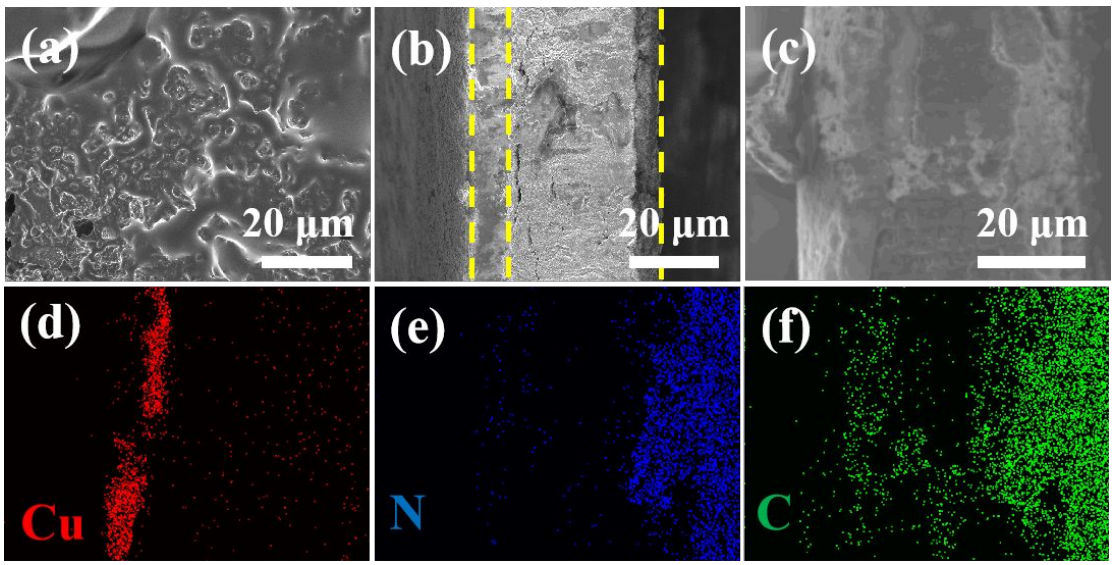

Figure S7. SEM image (a, b) and element mapping images (c-f) of the cross section of P-G-Cu after depositing 5 mAh cm^{-2} of Li.

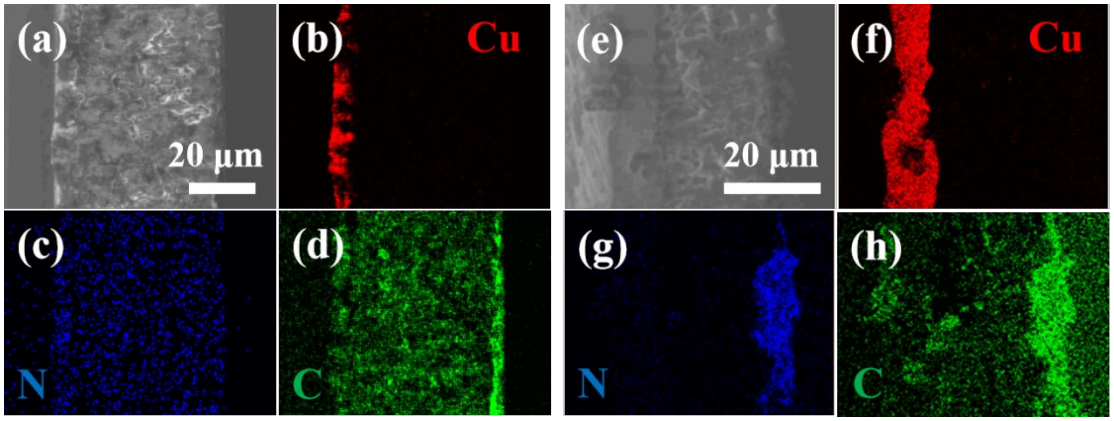

Figure S8. SEM images and element mapping images of the cross section of Cu (a-d) and A-G-Cu (e-h) after depositing 5 mAh cm^{-2} of Li.

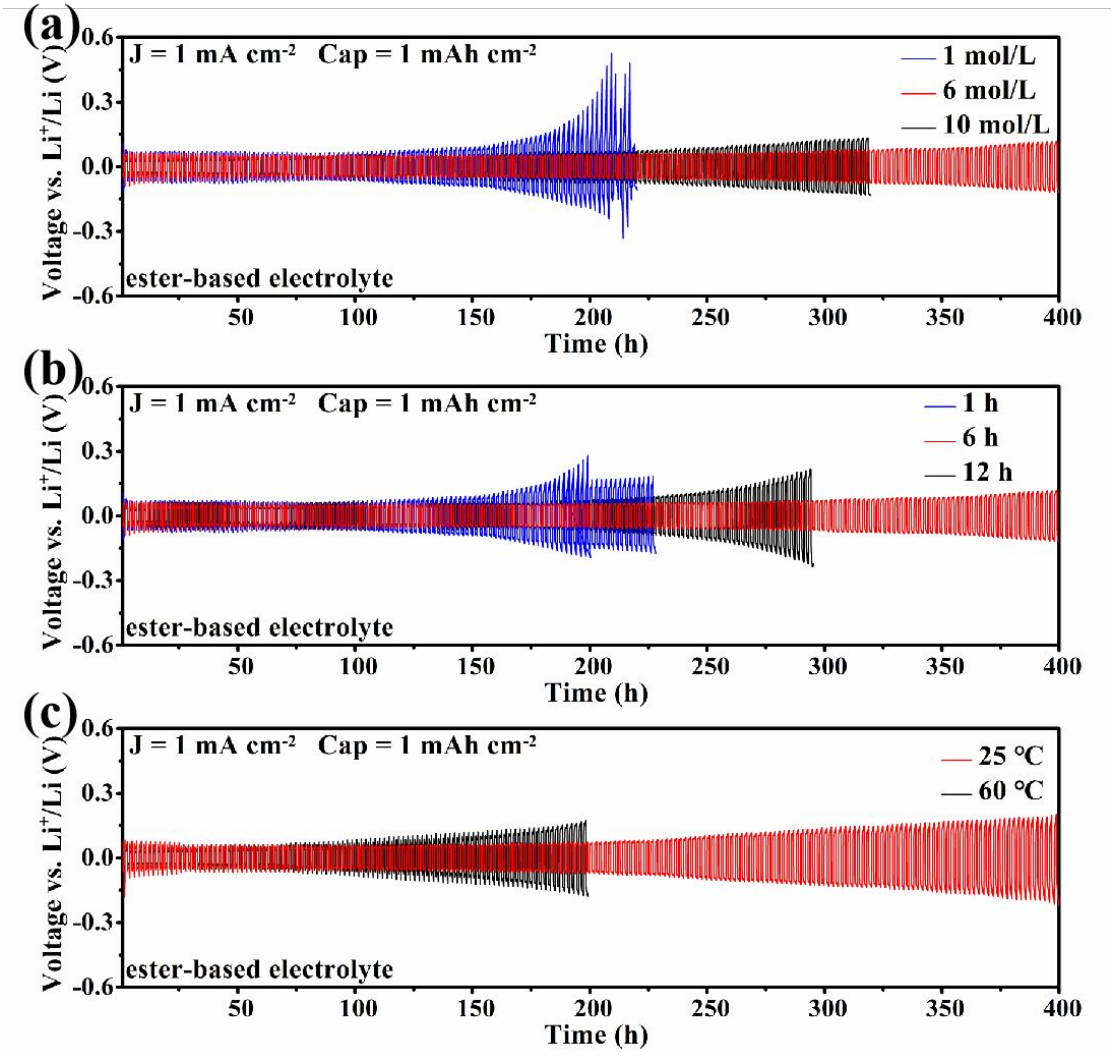

Figure S9. Cycling performance of the symmetric cells at 1 mA cm^{-2} with a fixed capacity of 1 mAh cm^{-2} with A-G interface layers obtained at different treating conditions: (a) acidity, (b) time, and (c) temperature.

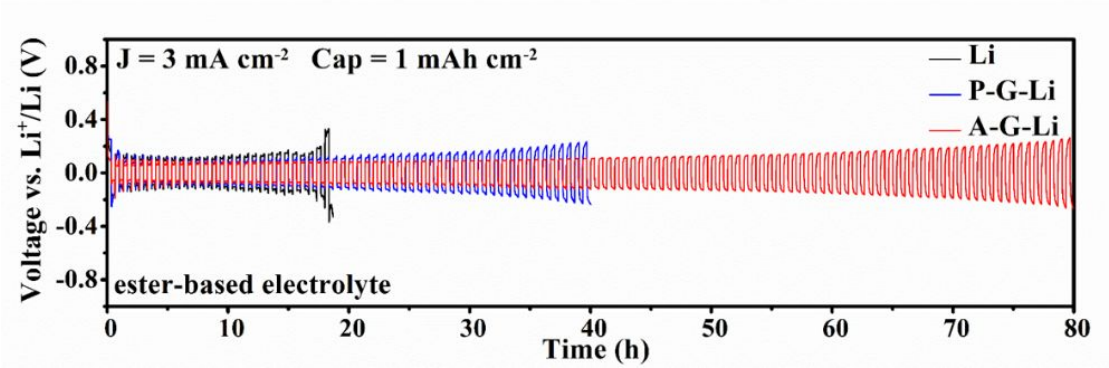

Figure S10. Cycling performance of the symmetric cells at 3 mA cm^{-2} with a fixed capacity of 1 mAh cm^{-2} in ester-based electrolyte.

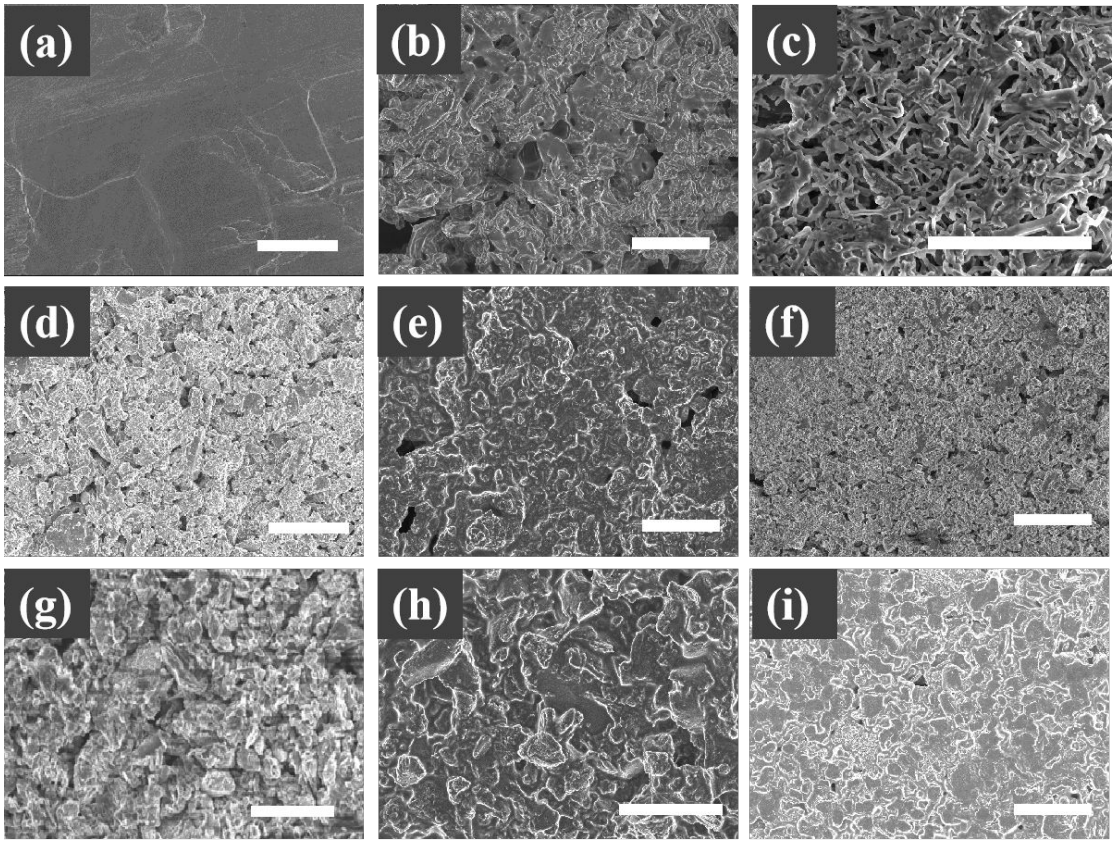

Figure S11. SEM images of pristine Li, P-G-Li and A-G-Li electrodes before cycling (a, d, g), after cycling at 1 mA cm^{-2} for 100 cycles (b, e, h), and after cycling at 3 mA cm^{-2} for 50 cycles (c, f, i) with an areal capacity of 1 mAh cm^{-2}. Ester-based electrolyte was used in these cells. The scale bar is 10 μm.

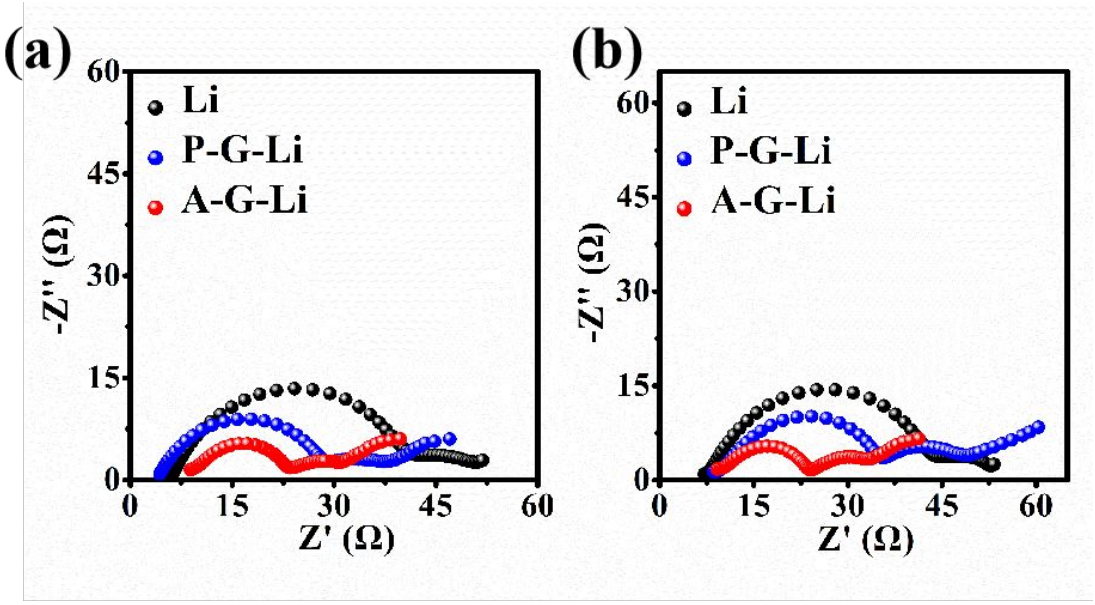

Figure S12. EIS spectra of symmetric cells with pristine Li, P-G-Li and A-G-Li electrodes after 10 cycles (a) and 50 cycles (b).

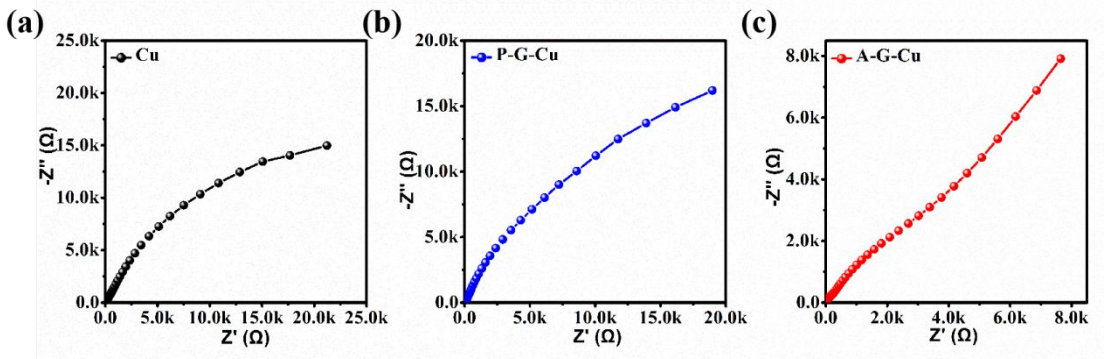

Figure S13. Nyquist plots of the asymmetric cells: (a) Li//Cu, (b) Li//P-G-Cu, and (c) Li//A-G-Cu. The Warburg impedance (Z_w) in the low-frequency range was ploted as a function of $\omega^{-1/2}$ for the estimation of the Li ion diffusion coefficient as shown in Figure 3e.

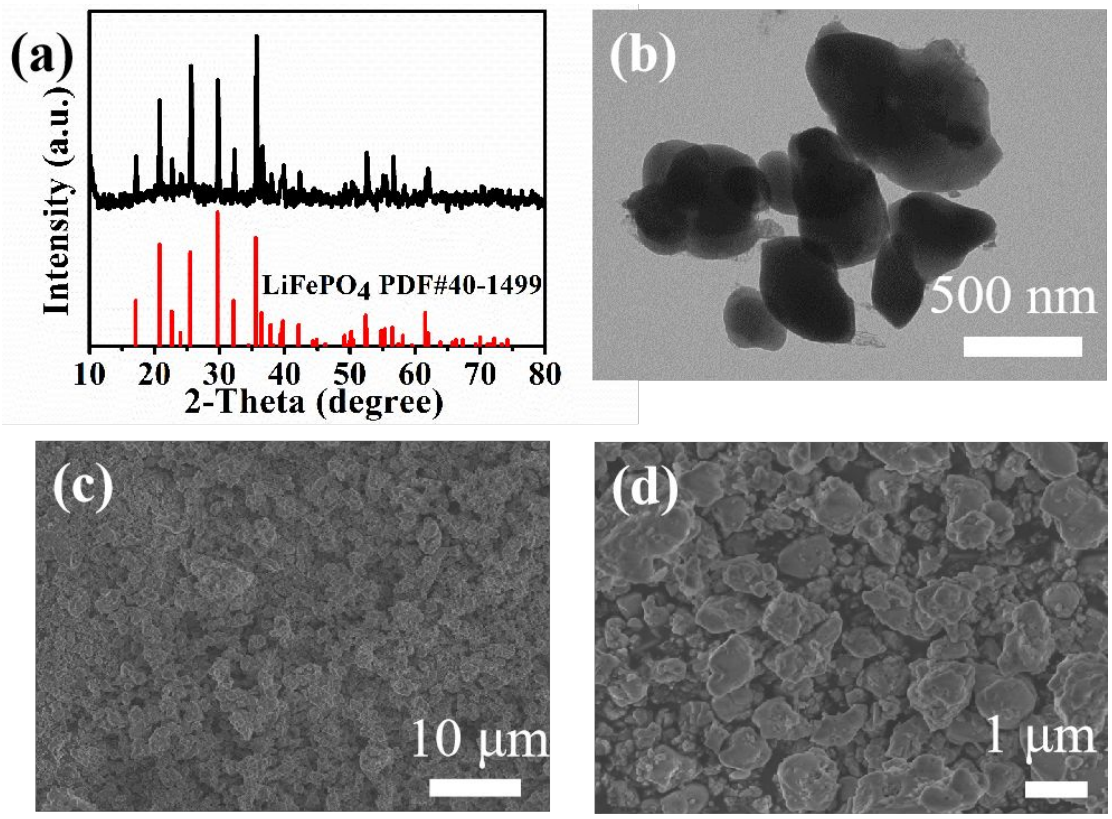

Figure S14. (a) XRD pattern, (b) TEM image and (c, d) SEM images of $LiFePO_4$.

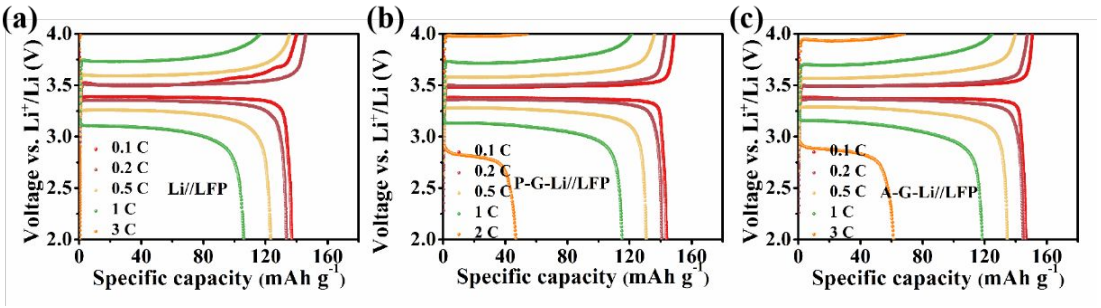

Figure S15. Voltage profiles of the Li//LFP full cells with (a) pristine Li, (b) P-G-Li and (c) A-G-Li anodes at different current densities.

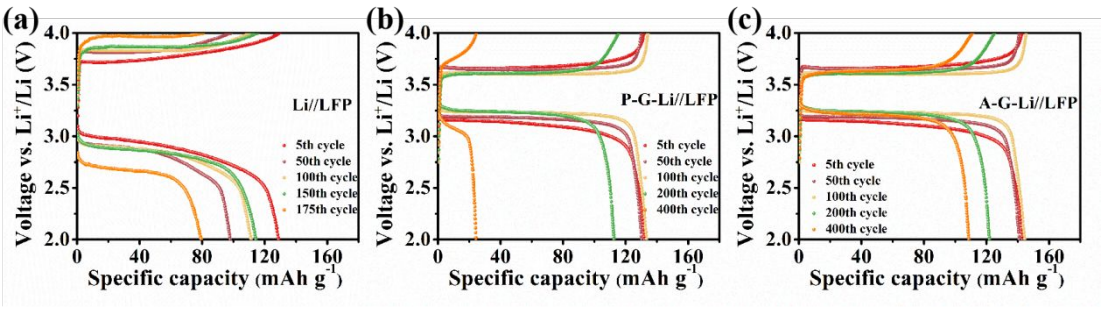

Figure S16. Voltage profiles of the Li//LFP full cells with (a) pristine Li, (b) P-G-Li and (c) A-G-Li anodes at different cycles.

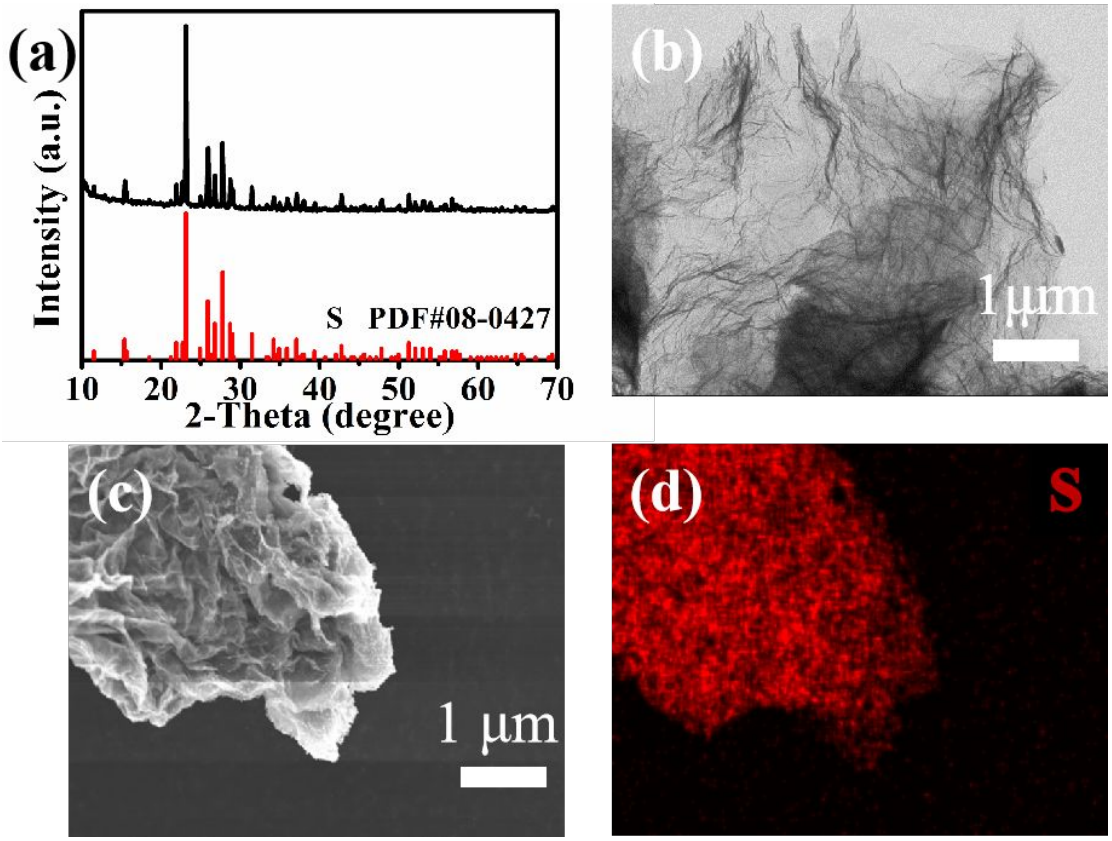

Figure S17. (a) XRD pattern, (b) TEM image, (c) SEM image, and (d) element mapping image of S/graphene composite.

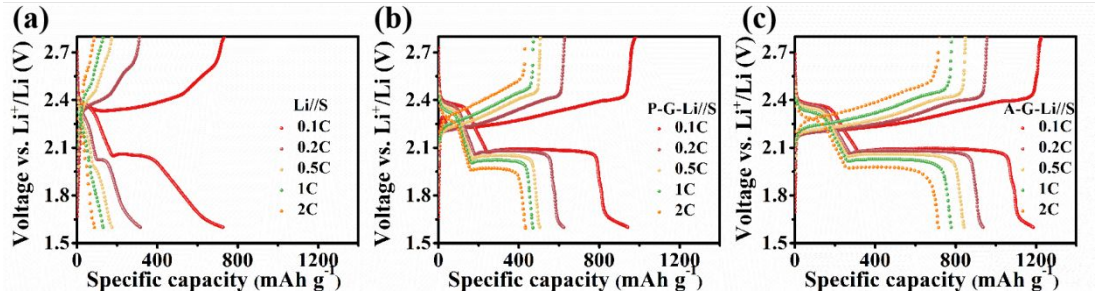

Figure S18. Voltage profiles of the Li//S full cells with (a) pristine Li, (b) P-G-Li and (c) A-G-Li anodes at different current densities.

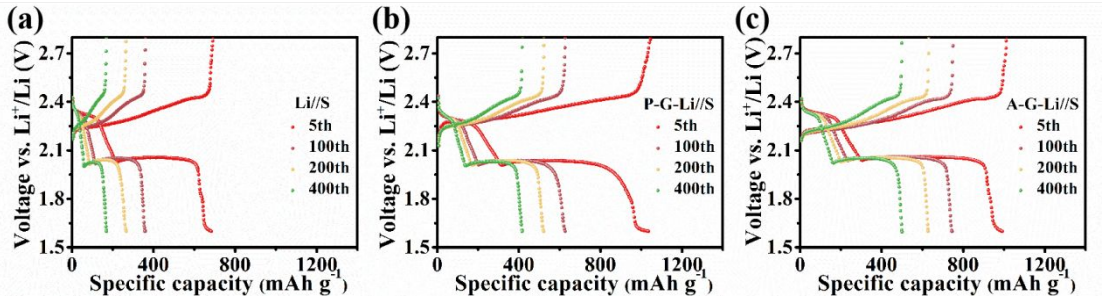

Figure S19. Voltage profiles of the Li//S full cells with (a) pristine Li, (b) P-G-Li and (c) A-G-Li anodes at different cycles.

Table S1. Fitting results of the EIS spectra in Figure 3 and Figure S12.

		Rs (Ω)	Rsf (Ω)	Rct (Ω)
OCV	A-P-Li	2.9	89.3	
	P-G-Li	12.4	94.2	
	Li	3.3	127.5	
10th cycle	A-P-Li	8.4	15.8	7.1
	P-G-Li	3.5	20.4	20.5
	Li	6.0	36.4	7.3
50th cycle	A-P-Li	8.7	16.2	7.3
	P-G-Li	8.8	29.2	10.6
	Li	7.3	36.6	7.5